

Investigation of critical-angle ultrasonic phenomena by Bragg diffraction of laser light

John P. Powers and Robert D. Brown Jr.

Department of Electrical Engineering, Naval Postgraduate School, Monterey, California 93940
(Received 11 July 1974)

A laser beam probe is used to study ultrasonic phenomena at a liquid-liquid interface. In particular, the technique has been used to detect and quantify evanescent waves generated at such an interface when the critical angle of incidence is exceeded. A mathematical description of the properties of evanescent waves is also given.

Subject Classification: 35.65.

INTRODUCTION

This paper describes the results of an investigation applying the principles of Bragg diffraction of laser light¹ by ultrasound to phenomena occurring at a liquid-liquid interface. The interface is insonified from the less dense medium, allowing the existence of a critical angle of incidence² at which all of the incident ultrasonic energy is reflected from the interface. A mathematical derivation is given to show that when the critical angle is met or exceeded, "evanescent" waves exist beyond the interface. These evanescent waves have wavelengths that are functions of the angle of incidence and amplitudes that decay exponentially in a direction normal to the interface. Experimental detection and measurement of the evanescent waves using a laser beam probe are described. Previous detection³ of evanescent ultrasonic waves of a fixed wavelength has been accomplished for an ultrasonic grating. However, the new experiment described gives greater flexibility in verifying the existence of evanescent wave because of the variable wavelength and decay rate. It provides an excellent visual demonstration of critical angle phenomena.

I. SUMMARY OF BRAGG DIFFRACTION PROPERTIES

Bragg diffraction¹ of laser light from ultrasound occurs when a laser beam passes through a comparatively wide sound field at the proper angle. When the angular alignment conditions⁴ between the incident light and sound are met, part of the light is diffracted out of the laser beam. It is noted that the alignment of the diffracted light and a determination of whether the diffracted light is upshifted or downshifted in frequency (another property of Bragg diffraction) indicate the propagation direction of the sound. The diffracted light is separated from the primary beam by an angle given by $\theta_B = \sin^{-1} \lambda / 2\Lambda \approx \lambda / 2\Lambda$, where λ and Λ are the wavelengths of light and sound, respectively. Hence the deflection angle of the diffracted light is sensitive to the wavelength of the ultrasound. It can be shown⁴ that the amplitude of the diffracted light is proportional to the amplitude of the ultrasound. This feature allows comparative measurement of ultrasound at different positions or moments in time provided that the ultrasonic frequency, the angular alignment, and incident light intensity remain constant. Techniques also exist to obtain

comparative phase measurements⁵; however, these were not used in our experiments. Summarizing the properties of Bragg diffraction and their applications to probing ultrasonic fields:

- (a) The angular alignment requirement can be used to select ultrasound traveling in certain directions and to discriminate against all other directions of propagation.
- (b) The alignment of the diffracted spots indicates the propagation direction of the ultrasound.
- (c) Deflection angle measurements indicate the wavelength of the ultrasound.
- (d) Intensity measurements of the diffracted light provide information about the comparative intensities (or amplitudes) of the ultrasound at different positions or times.

II. CRITICAL-ANGLE PHENOMENA

The situation to be analyzed is illustrated in Fig. 1. Two liquids of different densities ($\rho_2 > \rho_1$) form a liquid-liquid interface. The interface is insonified from the side of the interface with the lower acoustic velocity ($c_1 < c_2$) in the illustration. The angles θ_i , θ_r , and θ_t indicate the angles of incidence, reflection, and transmission and are measured with respect to the normal of the interface. Analysis of transmitted and reflected waves based on Snell's law and the boundary conditions is given in many elementary acoustics texts.² The results predict that as the angle of incidence is increased, θ_t becomes larger and that the transmitted amplitude will drop, with a corresponding increase in the reflected wave amplitude. When the angle of incidence reaches the "critical angle" [$\theta_c = \sin^{-1}(c_1/c_2)$], the angle of transmission reaches 90° and all of the incident energy appears in the reflected wave. An analysis is now given for the case where the critical angle is exceeded and will show that even though all energy is reflected, there does exist "evanescent" or "creeping" waves in the second medium. Expressions for the wavelength and exponential decay of these waves will be given for comparison with experimental results.

The following analysis will be limited to the case of ideal plane waves. Using the geometry of Fig. 1, equations for the incident, reflected, and transmitted pressure plane waves can be written as

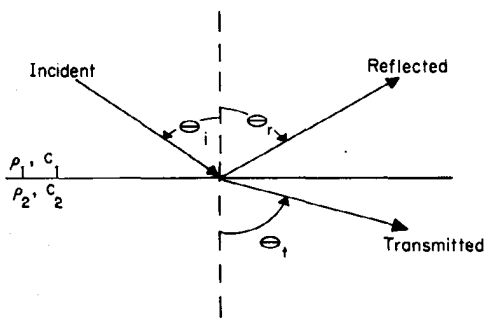


FIG. 1. Sketch of geometrical arrangement showing the incident, reflected, and transmitted rays.

$$\rho_i = A_1 e^{j(k_{ix}x + k_{iz}z)}, \tag{1}$$

$$\rho_r = B_1 e^{j(k_{ix}x - k_{iz}z)}, \tag{2}$$

$$\rho_t = A_2 e^{j(k_{tx}x + k_{tz}z)}, \tag{3}$$

where B_1 and A_2 are complex amplitudes (to account for any phase shift upon reflection or transmission). The quantities k_{ix} , k_{iz} , k_{tx} , and k_{tz} are the x and z components of the incident and transmitted propagation vectors, respectively. The fact that the angle of incidence equals the angle of reflection has been used in writing Eq. 2. Applying the conditions of continuity of pressure and velocity across the interface, the equations and the ratios B_1 and A_2 to A_1 can be written (as shown in Appendix A):

$$\frac{B_1}{A_1} = \frac{\cos \theta_i - (\rho_1/\rho_2)(\sin^2 \theta_c - \sin^2 \theta_i)^{1/2}}{\cos \theta_i + (\rho_1/\rho_2)(\sin^2 \theta_c - \sin^2 \theta_i)^{1/2}}, \text{ at } z=0, \tag{4}$$

$$\frac{A_2}{A_1} = \frac{2}{\frac{\rho_1}{\rho_2} \frac{1}{\cos \theta_i} (\sin^2 \theta_c - \sin^2 \theta_i)^{1/2} + 1}, \text{ at } z=0, \tag{5}$$

For the cases where $\theta_i > \theta_c$, the square roots in these expressions will become imaginary, implying that a phase shift will occur upon reflection or transmission. It is noted that $|B_1/A_1|^2 = 1$, which agrees with the fact that all incident acoustic energy will appear in the reflected beam. It is also noted that, in general, $|A_2/A_1| \neq 0$, indicating that the evanescent waves do exist below the interface.

In order to determine the wavelength of the evanescent waves it is noted that, since the interface cannot support a shear wave, the x -directed wavelength above the interface must be equal to the x -directed wavelength below the interface. As seen from the geometry of Fig. 1, the x -directed wavelength is given by

$$\Lambda_{2x} = \Lambda_1/\sin \theta_i = \Lambda_2 \sin \theta_c/\sin \theta_i. \tag{6}$$

It is noted that this wavelength is shorter (since $\theta_i > \theta_c$) than the wavelength of sound at the same frequency in medium 2.

Knowing the x -directed wavelength, we can now find the z component of the propagation vector

$$k_{2z} = (k^2 - k_{2x}^2)^{1/2} \tag{7}$$

$$= \left[\left(\frac{2\pi}{\Lambda_2} \right)^2 - \left(\frac{2\pi \sin \theta_i}{\Lambda_2 \sin \theta_c} \right)^2 \right]^{1/2} \tag{8}$$

$$= \frac{2\pi}{\Lambda_2} \left[1 - \left(\frac{\sin \theta_i}{\sin \theta_c} \right)^2 \right]^{1/2}. \tag{9}$$

Since $\theta_i > \theta_c$ for the case considered, k_{2z} is imaginary and can be written as

$$k_{2z} = j\alpha, \tag{10}$$

$$\alpha = \left[\left(\frac{\sin \theta_i}{\sin \theta_c} \right)^2 - 1 \right]^{1/2}. \tag{11}$$

When Eqs. 6 and 10 are substituted into Eq. 3, it is obvious that the transmitted wave (the evanescent wave) has the properties that it propagates in the $+x$ direction with a wavelength that is a function of the angle of incidence (given by Eq. 6) and decays in the $+z$ direction with a decay rate given by Eq. 11. The normalized initial amplitude of the evanescent wave just under the interface is given by Eq. 5.

It now remains to verify the existence and properties of the evanescent waves. Since Bragg diffraction of laser light offers a nonperturbing probe that is sensitive to propagation direction, wavelength, and sound intensity it offers an appropriate tool for the detection of these waves.

III. EXPERIMENT

Figure 2 shows the apparatus used in the experiment. Fifteen-megahertz sound was generated by a 2-in.-square quartz transducer and was directed at a variable angle upon an interface between water ($\rho = 998 \text{ kg/m}^3$; $c = 1481 \text{ m/sec}$) and turpentine ($\rho = 870 \text{ kg/m}^3$; $c = 1250 \text{ m/sec}$). The critical angle of incidence for such an interface is 57.6° . The beam of a 15-mW HeNe laser placed at different distances above and below the interface acted as a probe. Measurements of the position and intensity of the diffracted light provided the quantitative data. Figure 3 shows one pattern obtained when the probe was positioned above the interface. Bragg diffracted light from the incident ultrasonic beam is present. Figure 4 shows the results when the laser beam is oriented to simultaneously produce diffracted light from both the



FIG. 2. Side view of acoustic cell showing liquid-liquid interface and rotatable transducer.



FIG. 3. Diffraction spots obtained for incident ultrasound.

incident and the reflected ultrasound. The increase of reflected sound intensity and change of angle as the incident angle increased was qualitatively observed, but no quantitative data was taken for this case.

Figure 5 shows a typical result with the laser beam positioned just below the interface before the critical angle is exceeded. Figure 6 shows the locus of diffracted spot from the transmitted sound as the critical angle of incidence was increased. Up to the critical angle, the spot moved on an arc of constant radius about the central order spot. The intensity of the diffracted light decreased as expected. Figures 7 and 8 show results when the critical angle is exceeded; hence they are diffracted from the evanescent waves below the interface. As indicated in Fig. 6, the spots followed horizontal motion when the critical angle was exceeded corresponding to the changing wave predicted by the theory. Quantitative measurement of the differences of position in Figs. 7 and 8 predicted a difference of 0.9° in the angle of incidence. The measured change of angle was 1.0° . The observed change of intensity between the observed diffracted spots is due to both the angular dependence of Eq. 5 and the angular misalignment of the laser beam which was not realigned between the experiments to maximize diffraction efficiency.

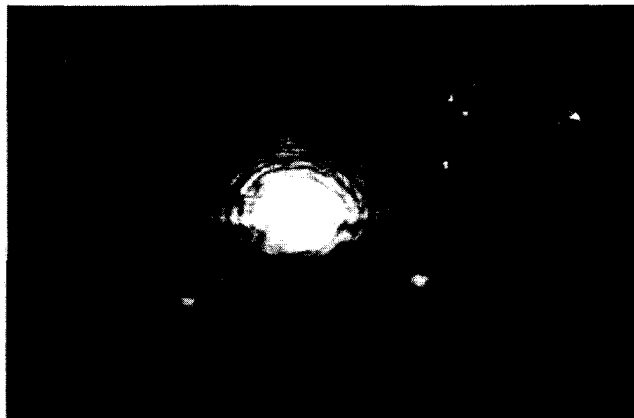


FIG. 4. Diffraction spots obtained simultaneously for incident and reflected ultrasound.

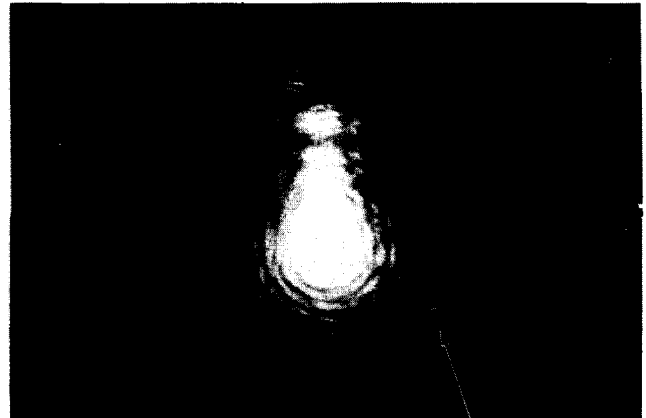


FIG. 5. Diffraction spot for transmitted ultrasound. (Liquid interface causes elongation of central order spot.)

Measurements were made with fixed angular alignment but at various distances beneath the interface to check the intensity dependence predicted by Eq. 11. The measured decay rate of $1.6 \times 10^{-3} \text{ m}^{-1}$ compares favorably with the predicted decay rate of $1.1 \times 10^{-3} \text{ m}^{-1}$.

IV. SUMMARY

These discussed experiments and measurements demonstrate the existence of evanescent ultrasonic waves and verify the wavelength and decay dependence as predicted by scalar wave theory. The properties of Bragg diffraction to measure the wavelength, amplitude and propagation direction of an ultrasonic wave with no perturbation of that wave were ideally suited for the desired measurements of the evanescent waves.

APPENDIX A

The derivation of Eqs. 4 and 5 from Eqs. 1, 2, and 3 follows. Continuity of pressure across the boundary at $z=0$ gives

$$A_1 e^{jk_1 x} + B_1 e^{jk_1 x} = A_2 e^{jk_2 x} \tag{A1}$$

Continuity of the normal velocity across the boundary gives

$$\frac{A_1}{\rho_1 c_1} \cos \theta_i - \frac{B_1}{\rho_1 c_1} \cos \theta_i = \frac{A_2}{\rho_2 c_2} \cos \theta_t. \tag{A2}$$

Solving simultaneously for B_1 ,

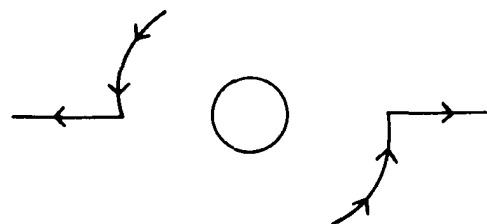


FIG. 6. Observed locus of diffraction spot for transmitted ultrasound for increasing angle of incidence.

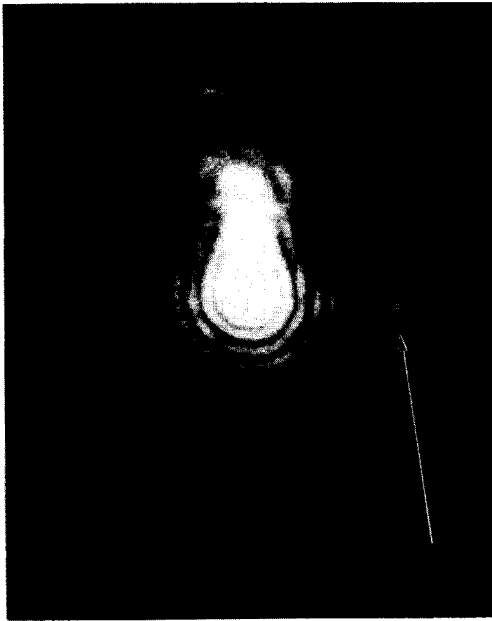


FIG. 7. Diffracted spot for evanescent wave for incident angle greater than the critical angle.

$$B_1 = A_1 \frac{\rho_2 c_2 \cos \theta_i - \rho_1 c_1 \cos \theta_t}{\rho_2 c_2 \cos \theta_i + \rho_1 c_1 \cos \theta_t} \quad (\text{A3})$$

$$= A_1 \frac{\cos \theta_i - (\rho_1 c_1 / \rho_2 c_2) \cos \theta_t}{\cos \theta_i + (\rho_1 c_1 / \rho_2 c_2) \cos \theta_t} \quad (\text{A4})$$

Since Snell's law is

$$\sin \theta_i = (c_2 / c_1) \sin \theta_t \quad (\text{A5})$$

and the critical angle is defined by

$$\sin \theta_c = c_1 / c_2, \quad (\text{A6})$$

then

$$\frac{c_1}{c_2} \cos \theta_i - \sin \theta_c \left(1 - \left[\frac{\sin \theta_i}{\sin \theta_c} \right]^2 \right)^{1/2} \quad (\text{A7})$$

$$= (\sin^2 \theta_c - \sin^2 \theta_i)^{1/2}, \quad (\text{A8})$$

and hence

$$\frac{B_1}{A_1} = \frac{\cos \theta_i - \frac{\rho_1}{\rho_2} (\sin^2 \theta_c - \sin^2 \theta_i)^{1/2}}{\cos \theta_i + \frac{\rho_1}{\rho_2} (\sin^2 \theta_c - \sin^2 \theta_i)^{1/2}} \quad (\text{A9})$$

It is noted that if $\theta_i > \theta_c$, then the numerator and denominator of Eq. A9 are complex conjugates and that there is a phase shift upon reflection. The magnitude of this phase shift δ is given by

$$\delta = 2 \tan^{-1} \frac{(\rho_1 / \rho_2) (\sin^2 \theta_i - \sin^2 \theta_c)^{1/2}}{\cos \theta_i} \quad (\text{A10})$$

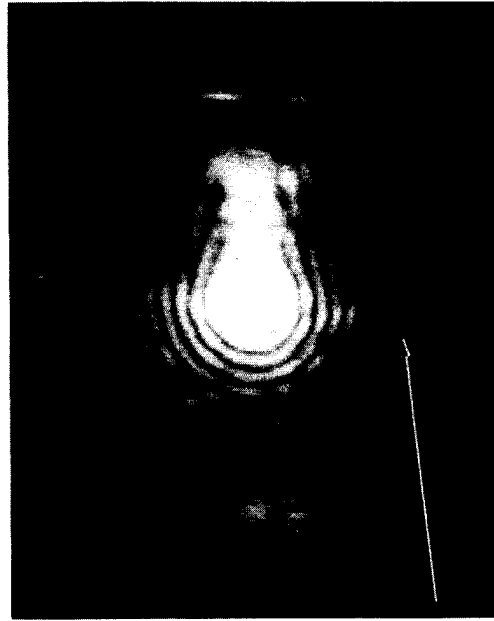


FIG. 8. Diffracted spot for evanescent wave incident at an even greater angle than Fig. 7.

Solving Eqs. A1 and A2 for B_2 gives

$$A_2 = A_1 \frac{2\rho_2 c_2 \cos \theta_i}{\rho_1 c_1 \cos \theta_i + \rho_2 c_2 \cos \theta_t} \quad (\text{A11})$$

$$= A_1 \frac{2}{1 + (\rho_1 c_1 / \rho_2 c_2) (\cos \theta_t / \cos \theta_i)} \quad (\text{A12})$$

Substituting for $c_1 \cos \theta_t / c_2$ as previously:

$$\frac{A_2}{A_1} = \frac{2}{1 + \frac{\rho_1}{\rho_2} \frac{1}{\cos \theta_i} (\sin^2 \theta_c - \sin^2 \theta_i)^{1/2}} \quad (\text{A13})$$

as expressed in Eq. 5. It is noted that, for $\theta_i > \theta_c$, there is both a change of magnitude and a phase shift encountered in traversing the boundary. As pointed out in the text, the wave in medium two then decays exponentially with z (Eq. 10) and represents an evanescent wave.

¹R. Adler, IEEE Spectrum 4 (5); 52-54 (1967).

²L. E. Kinsler and A. R. Frey, *Fundamentals of Acoustics* (Wiley, New York, 1962), 2nd ed., pp. 128-150.

³G. Wade, J. P. Powers, and A. A. de Souza, J. Acoust. Soc. Am. 45, 1247-1250 (1969).

⁴M. G. Cohen and E. I. Gordon, Bell Syst. Tech. J. 44(4), 693-721 (1965).

⁵A. Korpel, L. W. Kessler, and M. Ahmed, J. Acoust. Soc. Am. 51, 1582-1591 (1972).